Available online at https://sej.journals.ekb.eg/

FACULTY OF ENGINEERING – SOHAG UNIVERSITY

Sohag Engineering Journal (SEJ) VOL. XX, NO. XX, Month 20XX

Approaching Index Switching Algorithm for Position Control of a Single-Joint Robotic Arm

Ahmed Abdel-Sattar[a,c*], Ahmed M. Kassem[a], Shehab R. Tawfeic[b], Abou-Hashema M. El-Sayed[c]

[a] *Department of Electrical Engineering, Faculty of Engineering, Sohag University, Sohag, Egypt.*

[b] *Mechanical Power Eng. Department, Faculty of Engineering, El-Minia University, El-Minia, Egypt.*

[c] *Department of Electrical Engineering, Faculty of Engineering, El-Minia University, El-Minia, Egypt.*

Abstract

This paper presents a novel control strategy, denoted as Approaching Index Switching Algorithm (AISA) developed to attain further improvements of speed and accuracy and reduce energy consumption in single-joint robotic arm control. AISA switches dynamically between a fast-acting proportional controller and a precise PID controller according to the operational state, based on an "approaching index." This switch logic enables performance optimization due to the quick response of the proportional controller, combined with the accuracy and stability of the PID controller. Particle Swarm Optimization was used to ensure good parameter tuning. The performance of AISA is verified by simulations in MATLAB Simulink based on a mathematical model of a single-joint robotic arm. Similar comparative performance studies were performed with conventional PID, optimal PID, fractional-order PID, and adaptive PID controllers. The results showed that the settling time, rising time, accuracy, energy consumption, and overall efficiency in control problems were obtained faster than AISA. Besides experimental validation, this experimental validation tested this method and indicated a possibility of good efficiency of AISA in robotic applications.

Keywords: Robotic arm– Approaching Index Switching Algorithm – PID —DC motors– optimization

1. INTRODUCTION

With the rise of robotic technology in different areas including welfare, medicine, and agriculture; more accurate control systems to meet this demand are required [1–3]. For instance, multi-joint robots are widely required in many robotic applications such as 3 Degree of Freedom (DoF); while to the best of our knowledge, a single-joint robotic arm is still a basic crane part and has a very important role within robotics [4], because some applications only need different loads along one-degree freedom. It is the basic module for multi-joint robot control. Single-joint control can help us to understand not just single-joint dynamics but also low-level control structures widely applicable in more advanced robotic systems [5]. A robotic arm is a mechatronic system, which is typically composed of a series of rigid bodies (links) connected through joints. The joints are designed to allow only a single-type motion in either pure rotational or translational which are true kinematic chains that represent the minimum elements of the machine [6-7]. We consider the dynamics and control of each joint, with its own transfer function and actuation being independent of other joints. It defaults to check all the basic underpinning principles of control algorithms (e.g., Proportional-Integral-Derivative (PID) controllers,) which are mandatory for the development of a more sophisticated control system [8–9].

In the context of single-joint robotic arm control, Direct Current (DC) motors are widely used in various fields, including robotics, due to their simplicity, ease of operation, reliability, and cost-effectiveness. However, precise position control of DC motors is crucial in applications requiring high-precision control systems. The primary objective of a motor position controller is to interpret a signal representing the desired angle and then drive the motor to that specific position. Microcontrollers are effective tools for precisely controlling DC motors by processing and executing the desired position signals[10-12].

The control of a robust and accurate robotic control system has been an important research topic in the field of robotics for some time, with various control strategies being suggested that have already been implemented, although not all are guaranteed to work on industrial-grade robots. In so many studies single-joint robotic arm models are used to compare and analyze the performance of selective control algorithms. For, as in [13] the authors

performed a comparative study of PD, PI, and PID controllers for controlling a single joint in robots indicating the pros and cons of each controller. Likewise, in [4] the authors studied the simulation, modeling, and control problems linked to robot arms bringing information about their dynamical behavior and kinematic properties. Also, the authors of [14] investigated robotic arm modeling, simulation, and control while emphasizing the necessity to take flexibility in design into account in the context of a robotic arm. Also, in [15] the authors explored the modeling, stability analysis, and control for a flexible single-link robotic manipulator, providing insights into the best control strategy for controlling the tip position of robotic manipulators.

The discrete PID algorithms used for controlling the actuator joint angle position on robot arm bases have been also explored. For example, in [16] the authors demonstrated the effectiveness of a discrete PID algorithm in achieving precise position control of a robot arm. Moreover, in [17] the authors proposed the use of optimization algorithms, such as PSO (Particle Swarm Optimization), to tune PID controllers for improved performance in robotic arm control.

More advanced control schemes including fractional-order control and fuzzy logic are also considered in recent studies to achieve control of robotic arm systems. For example, [18] proposed a fuzzy logic supervisory control to position a 5 Degrees of Freedom (DOF) robot arm where the developed algorithm demonstrated effective performance in terms of accuracy and robustness. In [19], the position control of a 3-DOF arm manipulator was developed with a fractional-order PID controller and PSO algorithm. Moreover, a self-tuning fuzzy sliding mode controller was designed in [20] for controlling the 3-DOF articulated robotic manipulator and showed an ideal performance in terms of accurate position control.

Several other investigations have looked at the potential for using fractional-order adaptive control and optimal fuzzy-fractional Order PID (FOPID) control strategies in robotic arm systems. For instance, authors in [21] presented a fractional-order adaptive MRAC (model reference adaptive control) controller for precise position control of an industrial robot arm, while in [22] the authors recommended an optimal fuzzy-FOPID controller for trajectory tracking of a 3DOF robot manipulator. This highlights the potential to grow new control approaches for robotic arm systems which in turn provide high accuracy, flexibility, and robustness.

The selection of optimal controller parameters is crucial for achieving precise and stable control in engineering systems, and proper tuning of PID coefficients is essential for improving transient response parameters and steady-state accuracy [23]. To address various control challenges, advanced tuning methods like Particle Swarm Optimization are employed, which is a robust and modern optimization methodology that can identify the global optimal solution in a complex search space. PSO is widely used due to its straightforward implementation, cost-effectiveness, and high efficiency, and it has been inspired by the behavioral patterns of animals to address optimization problems, making it a popular choice for ensuring efficient, reliable, and robust system performance in diverse industrial applications[24].

This work was necessary due to the limits observed in existing industrial robotics control systems. Previous research has thoroughly explored a variety of control strategies, including standard PID, optimal PID, fractional-order PID, and adaptive PID controllers. While these tactics have produced useful results and improvements, they all have drawbacks. Standard PID controllers may fail to maintain stability and precision under changing load conditions, resulting in longer reaction times and higher power consumption. While optimal PID controllers are more effective, they require complex tuning methods and may fail to respond effectively to real-time system dynamics changes. Fractional-order PID controllers, while more control adaptable, are analytically expensive and difficult to implement in practical situations. Adaptive PID controllers, which update parameters in real-time, may have slow convergence rates and not always achieve the necessary accuracy. Given these drawbacks, there is an urgent need for a more resilient, adaptable, and economical control strategy. This work fills that gap by presenting the AISA, which dynamically changes between a proportional controller and a PID controller depending on real-time operating requirements, enhancing performance, and overcoming the limits of earlier control systems.

This article discusses the use of control strategies, particularly PID controllers, in controlling a single-joint manipulator, which opens possibilities of controlling more complex multi-joint systems. To quickly and accurately respond, an alternative switching control scheme is applied to a robotic arm that involves switching between two distinct controllers: a fast set-up proportional controller and the position termination PID controller. The primary advantage of this is the design of the new Efficient Approaching Index Switching Algorithm which increases the operational speed without compromising precision in mobile industrial robots [25],[26]. This breakthrough reveals a new complex switching strategy at dynamic range extending where control is changed from a proportional controller to a PID controller using an enhanced “approaching index” approach. Using detailed simulations and optimization of the parameters by way of MATLAB Simulink and Particle Swarm Optimization (PSO) respectively, the optimized AISA application techniques are more advanced than several other control techniques such as standard PID, optimal PID, fractional-order PID, and adaptive PID. It has been proven experimentally that in addition to other control techniques, the optimized AISA settles and rises in the shortest though with the highest accuracy as well as efficiency without consuming too much energy unlike the conventional AISA making it a potent tool in the control of robotic arms.

This paper consists of seven main sections. The opening section serves as a brief introduction to the key ideas and relevance of robotic arms in various engineering sectors. Section 2 provides a careful analysis of the system

dynamics through mathematical modeling to illustrate system parts relationships. A succinct description of the control model being addressed is attained in Section 3. This includes how it is implemented, the parts it comprises, and how it operates. Section 4 navigates the determining optimal features of the forecasted control method and makes use of optimization techniques. The simulation results and discussion are presented in Section 5, and this further has four subheadings: 5.1 gives details of the performance of Conventional PID and Approaching Index Switching Algorithm (AISA), 5.2 provides a comparison of Optimal PID performance and AISA, 5.3 Addresses the comparison of Fractional Order PID performance and AISA, 5.4 Provides a review on Model Reference Adaptive Control and AISA performance comparison, Section 6 explains the general context of the system as well as the designs and step by step procedures employed in the practical work aimed at validation of the simulated findings results. Lastly, Section 7 contains the overall conclusion of the research, describing the main aspects and outcomes of the study.

2. SYSTEM DYNAMICS

Mathematical modeling of robot manipulators is a method to describe the behavior of robot manipulators and to determine the relationship between joint position and velocity to torque/force or current/voltage. Mathematical modeling can also be used to describe the dynamic effects (e.g., inertia, centrifugal, and other parameters) on the behavior of the system. In such a robotic arm, a DC motor is preferred because of its excellent control of speed. The electrical model of such a DC motor is shown in Fig. 1.

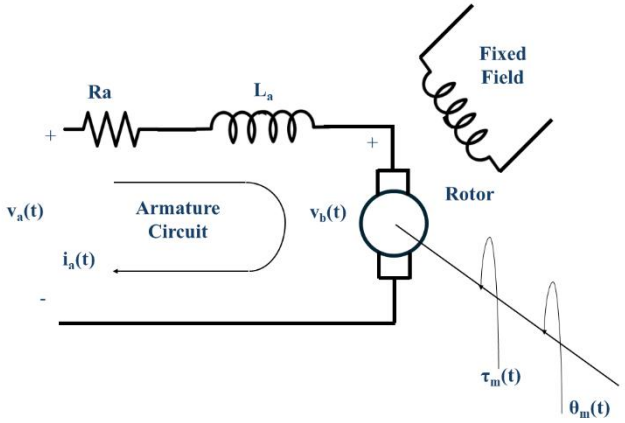

Fig. 1. Fixed-field DC motor circuit diagram.

To start modeling the robotic arm, we consider a single-joint robotic arm connected to a fixed field-DC motor. The back Electro-Motive Force (back-EMF) is induced by the armature winding of the DC motor by rotation in the magnetic field, and the generated EMF is proportional to the speed of the motor as follows [27]:

$$v_b(t) = k\omega_m = k_b \frac{d\theta_m}{dt} \tag{1}$$

Where, $v_b(t)$ is the back EMF, measured in volts (V), ω_m is the speed of the motor, measured in radians per second (rad/s), θ_m is the angular position of the motor, measured in radians (rad), and k_b is the back EMF constant, measured in volt-second per radians (V·s/rad).

Applying KVL (Kirchhoff's Voltage Law) on the armature circuit of the DC motor

$$L_a \frac{di}{dt} + R_a i = e_a(t) - k_b \frac{d\theta_m}{dt} \tag{2}$$

Where, $e_a(t)$ is the armature voltage or the input voltage, measured in volts (V) supplied by the controller to the DC motor. R_a is the armature resistance of the motor, measured in ohms (Ω), L_a is the inductance of the motor, measured in Henry (H).

Taking Laplace transformation and rearrangement, we obtain:

$$I_a(s) = \frac{E_a(s) - k_b s\, \theta_m(s)}{R_a + L_a s} \tag{3}$$

The torque developed by the motor is proportional to the armature current as follows:

$$T_m = k_t i_a \tag{4}$$

Where, T_m is the developed torque by the motor, measured in newton-meters (N·m), i_a is the armature current, measured in amperes (A), k_t is the torque constant, measured in newton-meters per ampere (N·m/A). When performing energy balance, the sum of all tor-ques must equal zero:

$$T_m - T_{load} - T_{inertia} - T_{friction} = 0 \tag{5}$$

Substituting T_m, $T_{inertia}$, and $T_{friction}$ in Eq (5) gives

$$K_t i - T_{load} - J_m \left(\frac{d^2\theta_m}{dt^2}\right) - b_m \left(\frac{d\theta_m}{dt}\right) = 0 \tag{6}$$

Where T_{load} is the load torque, J_m is the motor inertia, measured in kilogram meters squared (kg·m^2), b_m is the motor friction, measured in newton-meters per radians per second (N·m·s/rad), and θ_m is the joint position. Taking Laplace transform and rearranging

$$k_t I(s) = (J_m s + b_m) s\theta_m(s) \tag{7}$$

Substituting Eq (3) in Eq (7), yields:

$$G_m(s) = \frac{\theta_m(s)}{E_a(s)} = \frac{k_t}{s[(R_a + L_a s)(J_m s + b_m) + k_b k_t]} \tag{8}$$

The load torque contribution is incorporated into the equivalent inertia J_{eqv} and equivalent damping b_{eqv} parameters. This approach accounts for the load's impact on the system dynamics without explicitly stating the load torque in the model. By absorbing the load torque into these equivalent parameters, the model is simplified while preserving the load's effects on the system.

The total equivalent inertia, including both the load and motor inertia, is

$$J_{eqv} = J_m + \frac{J_{load}}{n^2} \tag{9}$$

Where J_{load} is the load inertia, n is the gear ratio, and b_{load} is the load damping. The total equivalent damping is

$$b_{eqv} = b_m + \frac{b_{load}}{n^2} \tag{10}$$

The final form of the transfer function of a single-joint robot arm is

$$G_m(s) = \frac{k_t\, n}{L_a J_{eqv} s^3 + \left(R_a J_{eqv} + b_{eqv} L_a\right) s^2 + (R_a b_{eqv} + k_t k_b) s} \tag{11}$$

The transfer function of the robotic arm system gives us a relation between the input voltage to the motor and the desired position of the motor as an output of the system [4]. The simulations were performed using MATLAB/Simulink version 2020a, developed by The MathWorks, Inc., Natick, Massachusetts, USA, and the robotic arm's physical parameters are listed in Table 1.

TABLE 1. SINGLE-JOINT ROBOTIC ARM PARAMETERS

Parameter	Value	Explanation
R_a	1 Ω	Armature Resistance
L_a	0.23 H	Armature Inductivity
J_m	0.02 kg·m^2	Motor Mechanical Inertia
b_m	0.03 N·m·s/rad	Friction Coefficient
k_t	0.023 N·m/A	Motor Torque Constant
k_b	0.023 V·s/rad	Back EMF Constant
n	1	Gear ratio
m	1 kg	Arm Mass
l	40 cm	Arm length

3. THE APPROACHING INDEX SWITCHING MECHANISM

This research proposes an optimal approaching index switching algorithm that is used to improve the performance of a single-joint robotic arm. Furthermore, the effectiveness of the proposed method is compared with other techniques (i.e., conventional PID, optimal PID controllers, fractional order PID, and adaptive PID). The AISA is designed to control dynamic systems by using a switching control mechanism that alternates between two control structures. This approach helps in efficiently reaching the desired set value with minimal overshot and faster settling time.

The AISA simulates a robotic arm control system, the robotic arm goes at high speed toward its desired position, and when it approaches the desired position, the controller reduces the robotic arm's speed and then stops it at the desired position. The algorithm uses a closed-loop index to calculate the closeness of reaching the predefined position. The approaching index ε(t) is calculated simultaneously, and it helps in selecting the suitable controller for this stage. Mathematically ε(t) is represented in equation 12, where e(t) is the error signal at time t and Δr is the required change in the reference set value. The index ε(t) starts at 1 and moves towards 0 as the system reaches the required setpoint [25],[26].

$$\boldsymbol{\varepsilon(t) = \frac{e(t)}{\Delta r}} \tag{12}$$

The switching mechanism is based on comparing the index ε(t) with preset threshold value ε_s where, ($0 < \varepsilon_s < 1$). The system starts with a closed-loop p controller used for achieving fast response. Then when $\varepsilon(t) \leqslant \varepsilon_s$, the system switches to the closed-loop PID controller to achieve the required precision of the destination. The decision to switch a controller is expressed as:

$$\begin{aligned} &P\ controller\ on, && \varepsilon(t) \geq \varepsilon_s \\ &PID\ Contoller\ on, && \varepsilon(t) < \varepsilon_s \end{aligned} \tag{13}$$

The construction of AISA in this study consists of two controllers, the first arrangement is a closed-loop proportional controller, and the other is a closed-loop PID controller. Furthermore, Fig. 2 shows a block diagram of the switching algorithm in which the system is switched between proportional controller and PID controller structures. The advantages of AISA include faster settling time, minimal overshot, and control signal efficiency i.e. The control signal required is minimized, enhancing efficiency.

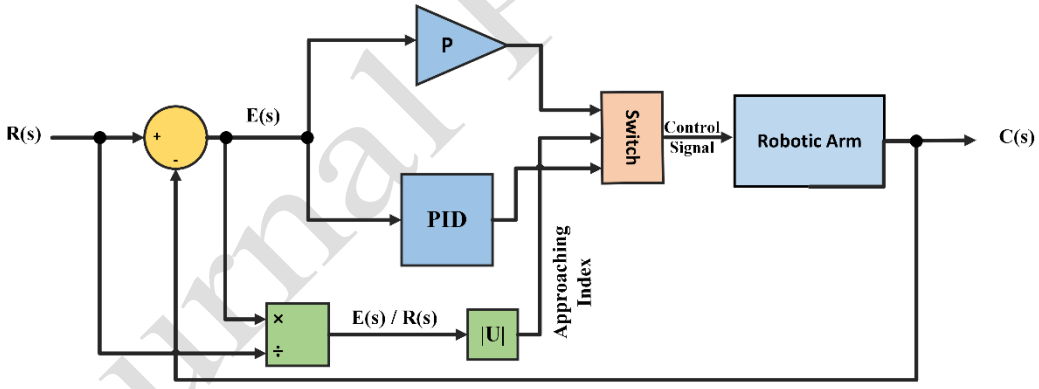

Fig. 2. Block diagram of the approaching index switching Controller.

where *R(s)* is the desired angular position, *E(s)* is the error signal and *C(s)* is the output signal.

A conventional PID controller has three fundamental parameters that require tuning: k_p is the proportional gain, k_i is the integral gain. and k_d is the derivative gain as shown in Fig. 3.

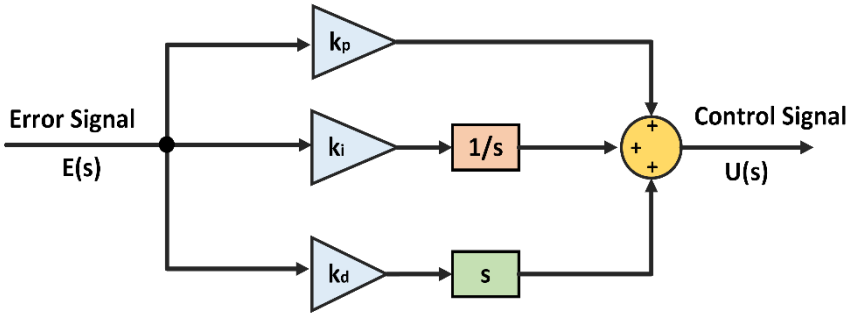

Fig. 3. Block Diagram of Proportional Integral Derivative (PID) Controller.

A PID controller can be represented as:

$$U(s) = (k_p + \frac{k_i}{s} + k_d s)E(s) \tag{14}$$

The PID controller and the robotic arm transfer functions are combined in a closed-loop system. The overall transfer function of the closed-loop system is given by:

$$G_{cl}(s) = \frac{G_{PID}(s)\, G_m(s)}{1 + G_{PID}(s)\, G_m(s)} \tag{15}$$

Where $G_{PID}(s)$ is the PID closed-loop transfer function The PID controller produces a control signal $U(s)$ to adjust the input to the robotic arm, reducing the error and improving the system's response. However, the derivative term in a PID controller can amplify high-frequency noise, which may cause problems in practical implementations, to address these issues the derivative term is often modified to include a low-pass filter, PID transfer function then becomes:

$$G_{PID}(s) = k_p\, s + \frac{k_i}{s} + k_d \frac{N}{1 + N\frac{1}{s}} \tag{16}$$

where N is the filter coefficient that determines the filter's cutoff frequency.

There are many advantages that the Approaching Index Switching Algorithm (AISA) proposes in the control of robotic arm structures. The most important one is that this algorithm permits the switching between different control laws (P and PID) depending on the location of the system concerning the reference, therefore improving the stability and the response. Because of this, the AISA can adeptly control the system and reduce the overshoot as it nears the final position. Its intelligent strategies include using a less complex proportional controller when away from the set point and switching to a more complicated PID controller close to the target thus avoiding the system's unnecessary power consumption with AISA-designed controls. Such properties make AISA applicable in areas where quick response and accuracy are required.

Nonetheless, AISA has certain limitations that cannot be overemphasized. One of these drawbacks can be the difficulty in tuning the approaching index where an inappropriate choice might lead to excessive cleaning or poor control performance. Additionally, the number of controller switches when controllers are operating close to one another can cause chattering which in turn can strain physical systems when noise is present. The AISA approach is also likely to face challenges when applied in the presence of large model uncertainties thus making it less effective for systems that change parameters or have external disturbances.

4. SELECTING THE OPTIMAL PARAMETERS OF THE PROPOSED CONTROLLER

The particle swarm optimization (PSO) has been used to select the optimal parameters of the proposed AISA based on Controller gains P, k_p, k_i, k_d the approaching index threshold value ε_s, and all other controllers used in the comparison. The considered method uses the collective behavior of particles in a swarm to search for the optimal parameters of the proposed method. PSO is known for its high capability in finding optimal solutions efficiently, especially in complex, multi-dimensional spaces. Its simplicity, computational efficiency, and robustness make it well-suited for control parameter tuning, where swift convergence to optimal values is crucial. PSO has been widely applied to various optimization problems, demonstrating reliable performance in control system optimization tasks.[28].

The process of selecting the optimal parameters of the proposed method based on the PSO algorithm is shown in Fig. 4. The particles in the swarm are initialized with random positions and velocities, and their movements are guided by the best existing positions. The particles then update their positions based on their own experiences and the experiences of other particles in the swarm. This iterative process continues until the optimal solution is obtained, at which point the PSO algorithm converges to the optimal parameters of the controller [29]. Particle swarm optimization parameters used in this research are listed below in Table 2.

In control system design, various specialized objective or fitness functions are employed to evaluate controller performance. Notable among these are the Integral of Squared Error (ISE), Integral of Time-weighted Squared Error (ITSE), Integral of Time-weighted Absolute Error (ITAE), and Integral of Squared Time-weighted Absolute Error (ISTAE). These objective functions are specifically designed to assess the effectiveness of controllers in minimizing errors over time. Each criterion is related to the integral of the error signal, providing a quantitative measure of how effectively a system follows a desired trajectory or setpoint. By utilizing these objective functions, engineers can systematically tune control parameters to enhance system performance and stability [30].

The ITAE is the considered fitness criterion, which minimizes the absolute error multiplied by time. It reduces both the magnitude and duration of errors, balancing between fast response and minimal overshot as shown in equation 17.

$$ITAE = \int_0^\infty t \times |e(t)|dt \quad (17)$$

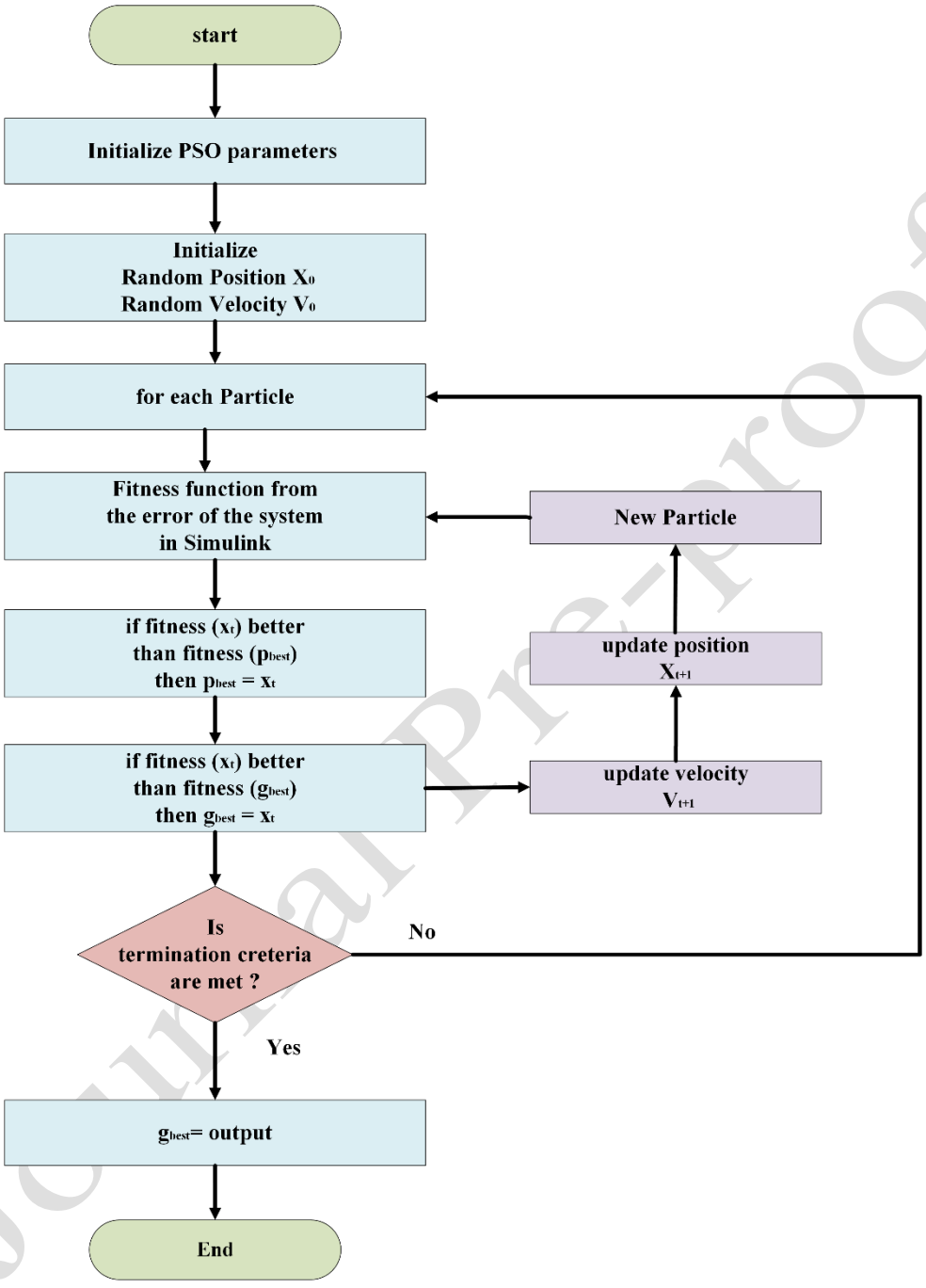

Fig. 4. Flow chart of Particle Swarm Optimization.

TABLE 2: PSO PARAMETERS

. Parameter	Value	Explanation
w	1.5	Inertia weight
w_{damp}	0.98	Inertia weight damping ratio
C_1	1	Personal Learning Coefficient
C_2	1	Global Learning Coefficient

5. SIMULATION AND RESULTS

In this section, the simulation of the robot model control was executed using the MATLAB Simulink tool, which relies on the mathematical model derived in the preceding section. The proposed method has been compared with various control techniques applied to the robotic arm model, and the resulting outcomes were systematically compared to evaluate their efficacy. Furthermore, Fig. 5 clears the considered scenarios to confirm the superiority.

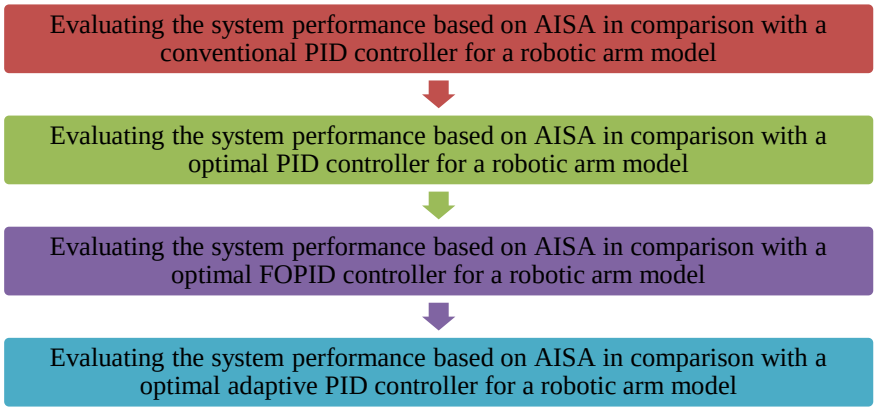

Fig. 5. The scenarios for the simulation results.

5.1. Evaluating the system performance of the AISA controller in comparison with a conventional PID controller for a robotic arm model

In this section, the performance of a robotic arm model was evaluated using the AISA in comparison with the conventional PID controller revealing significant advantages in terms of response time and accuracy. AISA's dynamic switching between two closed-loop control modes, based on the system's proximity to the target state or what we call the approaching index, allows for more efficient handling of the robotic arm's movements. As discussed previously, the AISA controller employs switching between two separate controllers: a P controller responsible for rapid response and the PID controller responsible for precision in achieving the desired output. Fig. 6. shows the Simulink model of the proposed technique.

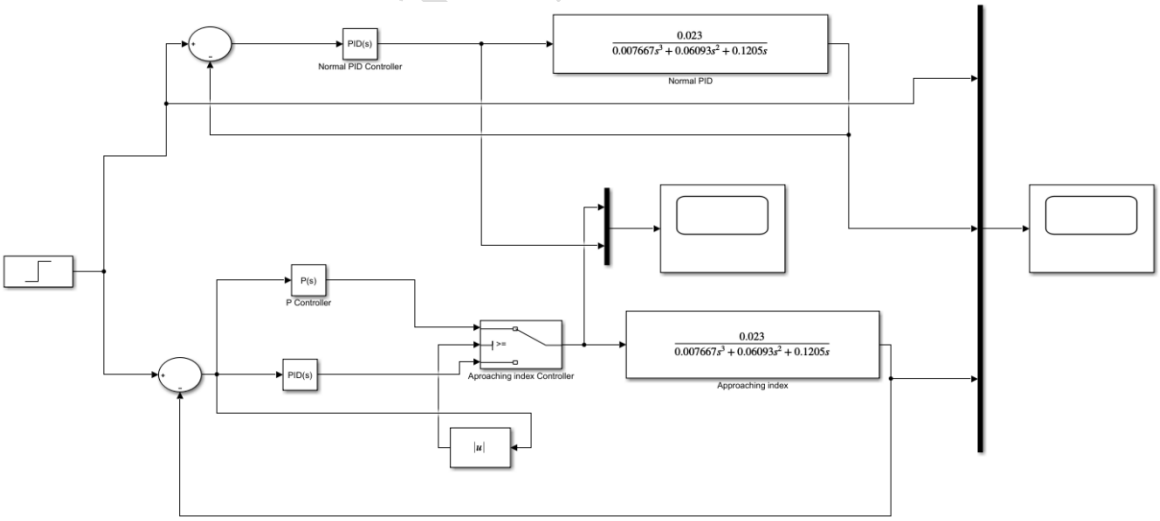

Fig. 6. Simulink model of the AISA controller versus the conventional PID controller.

The subsequent figures further illustrate the advantages of AISA over conventional PID controllers in these respects. Approaching Index Switching Algorithm (AISA) Parameters have been obtained from the PSO optimization process, and their upper and lower bounds are indicated in Table 3, for this simulation, the population size is 50, and the number of iterations is 100, considering the fitness function as ITAE.

TABLE 3: THE OPTIMAL PARAMETERS OF THE APPROACHING INDEX SWITCHING ALGORITHM.

. Parameter	Upper bound	Lower bound	Value
P	15	0	14
ε_s	1	0	0.777
k_p	15	0	5
k_i	5	0	0.01
k_d	5	0	1.85
N	100	0	29

Where P is the gain of the proportional controller, ε_s is the threshold value of the approaching index, k_p, k_i, and k_d are the parameters of the closed loop PID controller and N is the value of the filter coefficient.

To assess how well the control system works, angular position output, control signal, and error signal were obtained from two different tests performed on the system. Namely, the system was tested by a step signal and a square wave signal. More so, the conventional PID parameter settings have been provided in Table 4. The simulation results are presented in this section to analyze the behavior of the system towards different kinds of input variations. Fig. 7 demonstrates the angular position output of the active index switch controller and a conventional PID controller while using a step wave as reference input. The results show that the first controller is superior to the second controller, especially concerning rise time, settling time, and the absence of overshoot.

TABLE 4. CONVENTIONAL PID CONTROLLER PARAMETERS.

Parameter	Value
k_p	5
k_i	0.01
k_d	2
N	29

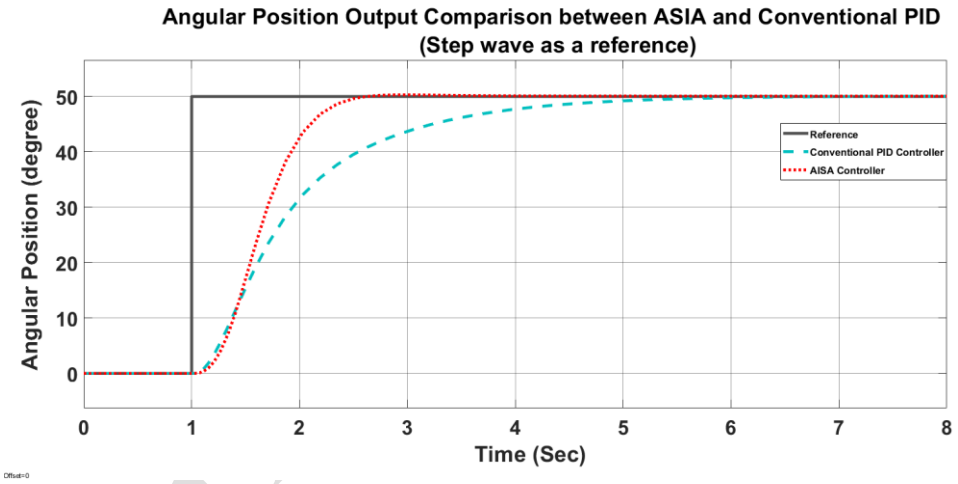

Fig. 7. The response for step input considering Conventional PID and AISA techniques.

Furthermore, Fig. 8 presents a comparative analysis of the system's angular position response under the application of a square wave as a reference input.

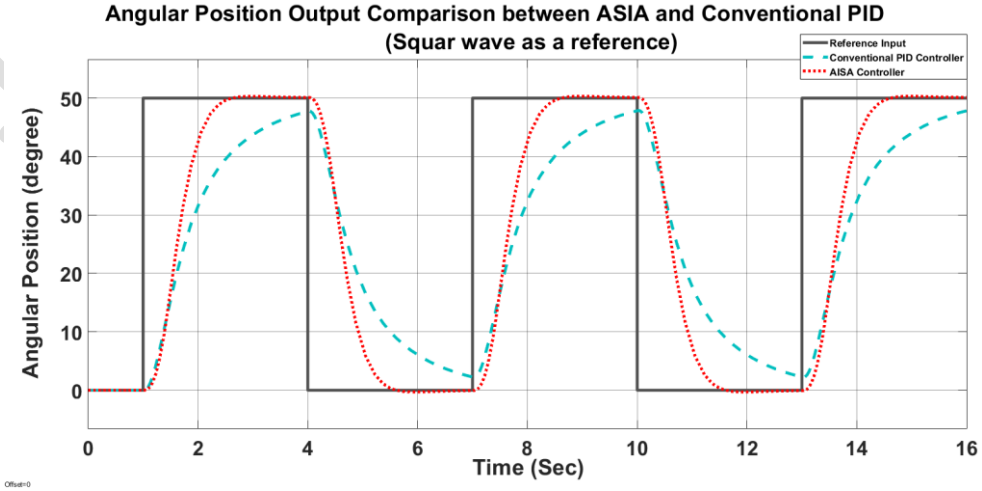

Fig. 8. The response for Square Wave input considering Conventional PID and AISA technique.

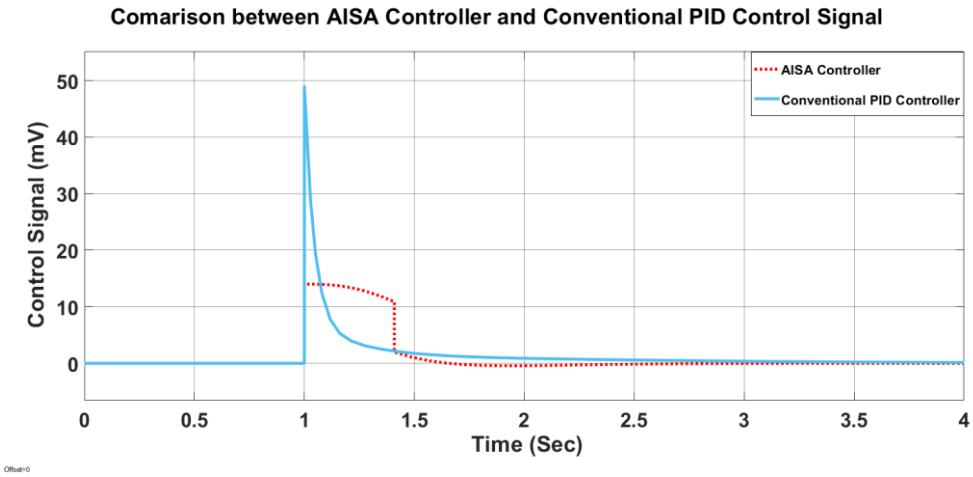

Fig. 9. The control signal considering Conventional PID and AISA techniques.

Moreover, Fig. 9 shows the control signal of the conventional PID controller. It appears relatively high at about (49 mV) for each angle degree; thus, the system requires a lot of power to achieve the required angular position. The system specifications (rise time, overshoot time, peak time, settling time) after using the PID control and the proposed AISA are presented in Table 5.

TABLE 5. SPECIFICATIONS OF THE AISA AND CONVENTIONAL PID SYSTEMS.

Specification	AISA	Conventional PID
Rise Time	0.81337 Sec	1.9984 Sec
Settling Time	2.4071 Sec	4.8752 Sec
Peak	50 degrees	50 degrees
Peak Time	2.8782 Sec	6.306 Sec

The results of the AISA-based systems in terms of quick settling times and decreased overshoot are an overall improvement in the accuracy of the arms placement. On the other hand, a conventional PID controller is successful in controlling the system, but many times suffer from overshot and longer settling times, especially in dynamic systems with load variations. Since AISA is fundamentally an adaptive controller, this increases its robustness in coping with these variations and thus provides stable and accurate performance. Therefore, the AISA control strategy is better than controlling robotic arms with PID controllers that are inefficient and unreliable.

5.2. Evaluating the system performance of AISA controller in comparison with an optimal PID controller for a robotic arm model

This part of the work makes a comparison of AISA with that of an optimal PID controller. In addition, the parameters of the optimal PID controller have been extracted from the execution of the PSO optimization process, and their maximum and minimum limits are presented in Table 6, for this simulation, the population size is 50, and the number of iterations is 100. Fig. 10 gives the Output angular position of systems for the PID based on PSO Algorithm Implementation which is ITAE Based. The ITAE criterion demonstrates the most preferable performance by achieving a balance in rise time while minimizing overshot margins.

TABLE 6: THE OPTIMAL PID CONTROLLER PARAMETERS

. Parameter	Upper bound	Lower bound	Value
k_p	15	0	5
k_i	5	0	0.05
k_d	5	0	5
N	100	0	58

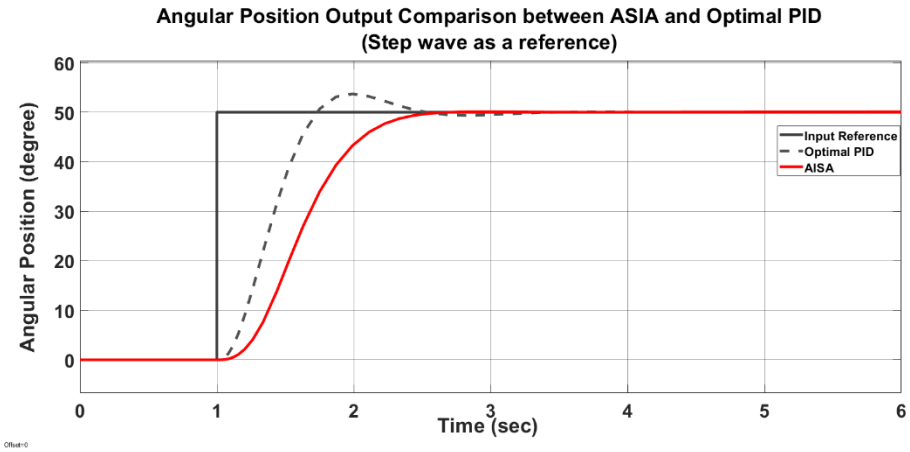

Fig. 10. The system response for step input considering optimal PID and AISA technique.

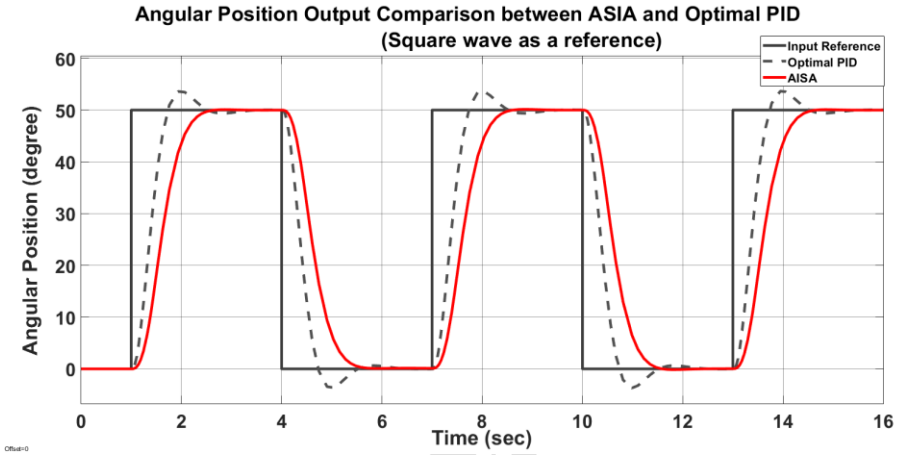

Fig. 11. The system response for Square Wave input considering optimal PID and AISA technique.

Further, the simulation was performed again with a square wave input and the outcome is displayed in Fig. 11, which narrates the response of the system to this specific input condition in depth. On the other hand, Fig.12 shows the control signal of the optimal PID controller and the AISA controller under consideration. The system characteristics (rise time, overshoot time, peak time, and settling time) achieved using the optimal PID control and the AISA controller are summarized in Table 7.

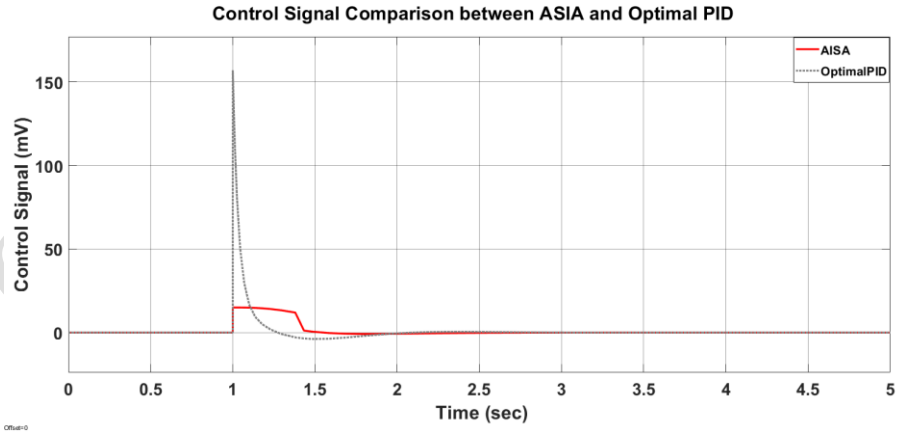

Fig. 12. The control signal considering optimal PID and AISA techniques.

TABLE 7. SPECIFICATIONS OF THE AISA AND OPTIMAL PID SYSTEMS.

Specification	AISA	Optimal PID
Rise Time	0.81337 Sec	0.4696 Sec
Settling Time	2.4071 Sec	2.5710 Sec
Peak	50 degrees	54 degrees
Peak Time	2.8782 Sec	2.0512 Sec

5.3. Evaluating the system performance of the AISA controller in comparison with a Fractional Order PID controller for a robotic arm model

FOPID represents an improved version of a PID controller that applies fractional calculus in extending the limits of the integral and derivative parts. In conventional PID designs, the integral and derivative components are both of an integer order (commonly 1 for their structure). In a FOPID controller, those orders may be expressed as real numbers, granting a wider scope for application and comparatively better performance in managing complicated systems such as a robotic arm [31], a block diagram of the FOPID controller is represented in fig.13. As stated previously in our research, we focused on the FOPID control technique for the simulation of a robotic arm model. The FOPID parameters have been obtained from the PSO optimization process, and their upper and lower bounds are indicated in Table 8, where λ is fractional integration order and μ is fractional derivative order, for this simulation the population size is 50 and the number of iterations is 100 and the considered fitness function is ITAE. A comparison between the FOPID control technique and the AISA control technique was performed and the angular position output in the case of using step input reference was shown in Fig. 14.

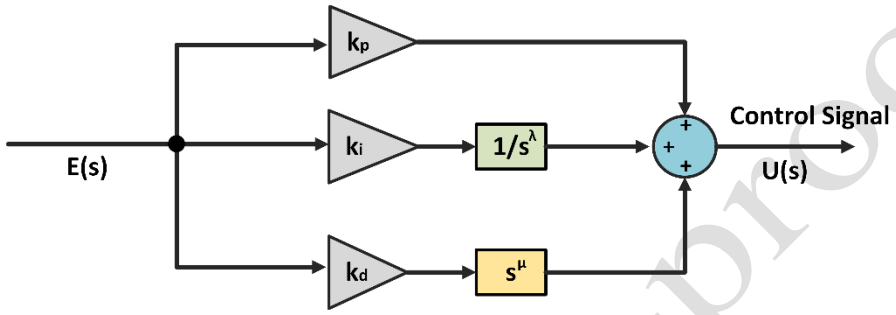

Fig. 13. Block diagram of the FOPID controller

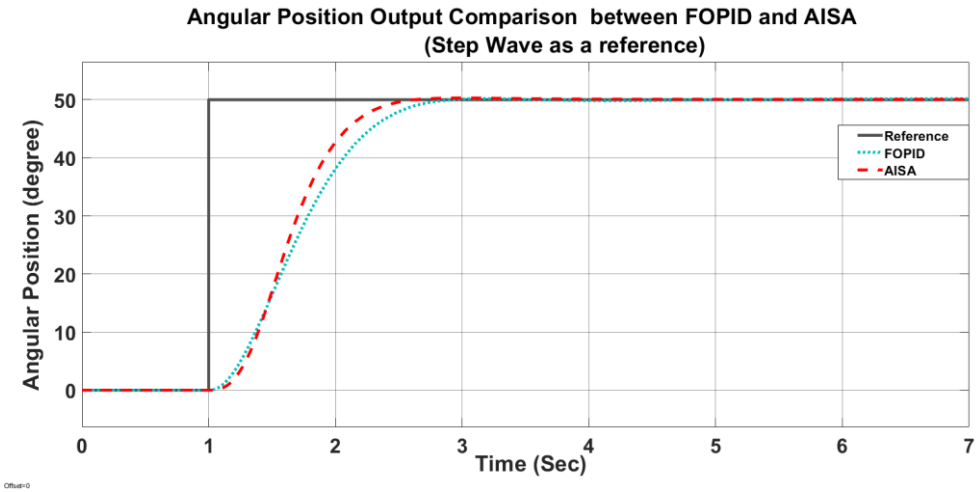

Fig. 14. The system response for step input considering FOPID and AISA technique.

TABLE 8: THE OPTIMAL PARAMETERS OF THE FOPID CONTROLLER.

. Parameter	Upper bound	Lower bound	Value
k_p	15	0	6.5
k_i	5	0	0.1
k_d	5	0	2
λ	1	0	0.75
μ	1	0	0.82

In Fig. 15, the simulation is repeated but square wave input is used as a reference.

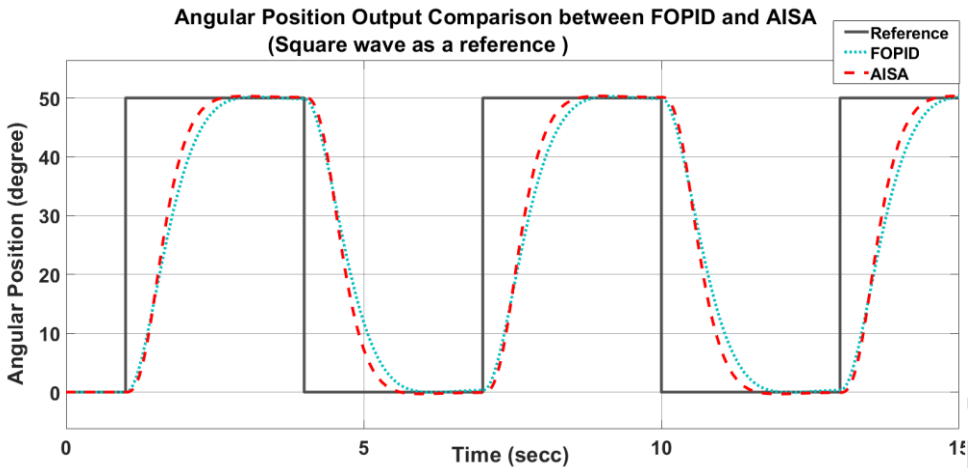

Fig. 15. The system response for Square Wave input considering FOPID and AISA technique.

The control signal formed by the AISA controller and FOPID controller is depicted in Fig. 16, AISA controller generates a smaller control signal than that of the FOPID controller as the data suggests. This indicates that the AISA controller is more power efficient.

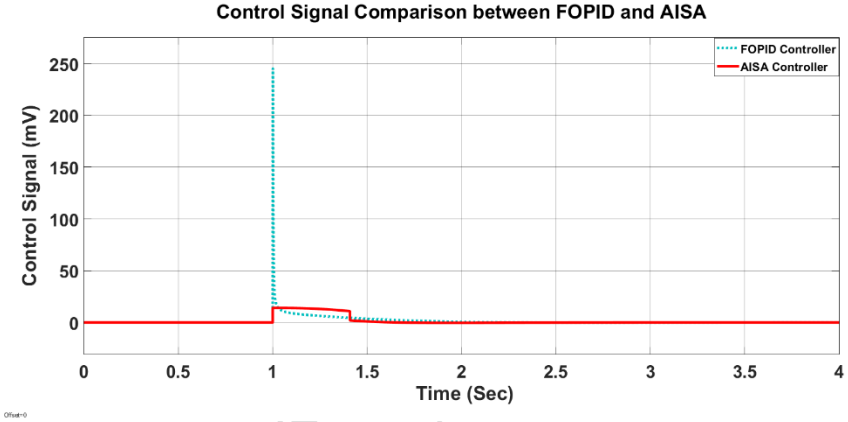

Fig. 16. The control signal considers optimal PID and AISA techniques.

In addition, Table 9 presents a comparative analysis of parameters for the robotic arm system with AISA and FOPID controller. It analyzes the performance in terms of time taken to rise, settle, and overshoot to see which control method is more effective. In this way, more useful information is provided about the performance and stability of the robotic arm in the different control strategies.

TABLE 9. SPECIFICATIONS OF THE AISA AND FOPID SYSTEMS.

Specification	AISA	FOPID
Rise Time	0.81337 Sec	1.0407 Sec
Settling Time	2.4071 Sec	3.0504 Sec
Peak	50 degrees	50 degrees
Peak Time	2.8782 Sec	3.3205 Sec

5.4. Evaluating the system performance of the AISA controller in comparison with the MRAC controller for a robotic arm model

In this section, the model reference adaptive control (MRAC) is considered a type of adaptive control strategy that adjusts the control parameters to ensure that the system's behavior follows a desired reference model [32], block diagram of the MRAC controller is shown in fig. 17. In this simulation, the MRAC technique based on the PID controller is used for position control of the robotic arm model. The optimal MRAC controller parameters have been obtained from the PSO optimization process, and their upper and lower bounds are indicated in Table 10, where γ is the adaptive gain or learning rate, the population size is 50, the number of iterations is 100 and the considered fitness function is ITAE. Fig. 18 and Fig. 19 demonstrate the angular position output in the case of using step and square wave inputs respectively.

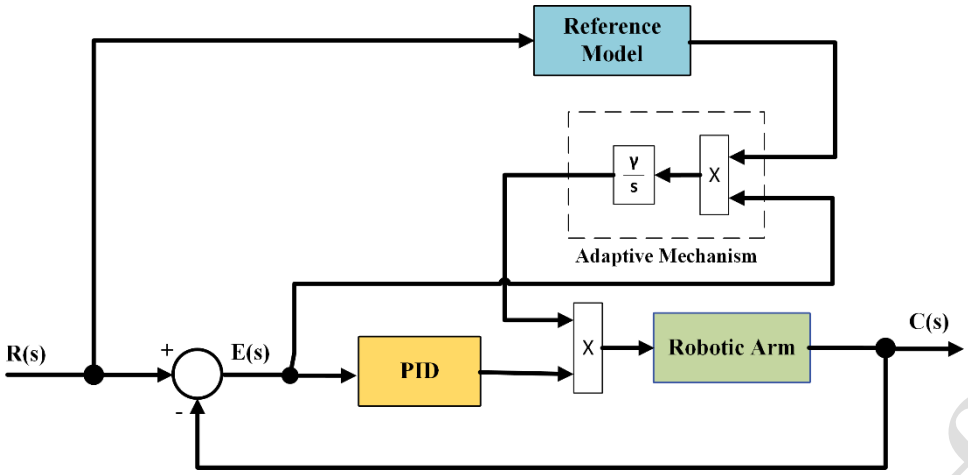

Fig. 17. Block diagram of the MRAC controller

TABLE 10: THE OPTIMAL PARAMETERS OF THE MRAC CONTROLLER.

. Parameter	Upper bound	Lower bound	Value
k_p	15	0	9
k_i	5	0	0.05
k_d	5	0	2
γ	1	0.001	0.1

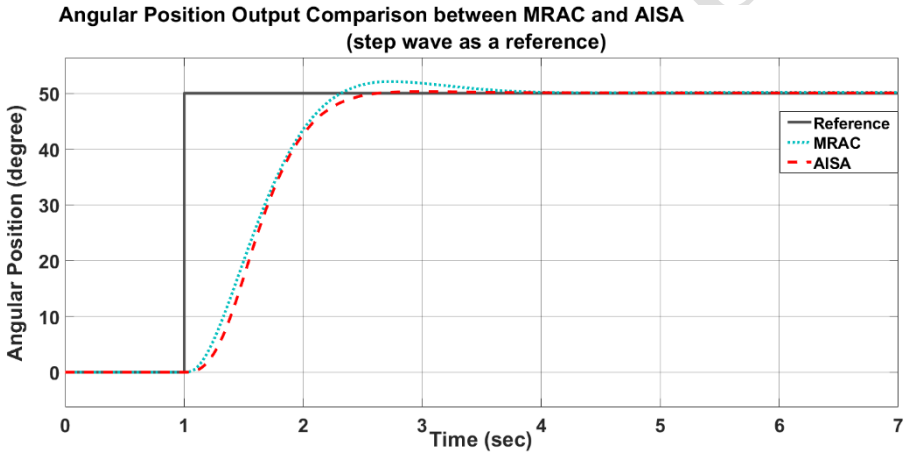

Fig. 18. The system response for step input considering MRAC and AISA techniques.

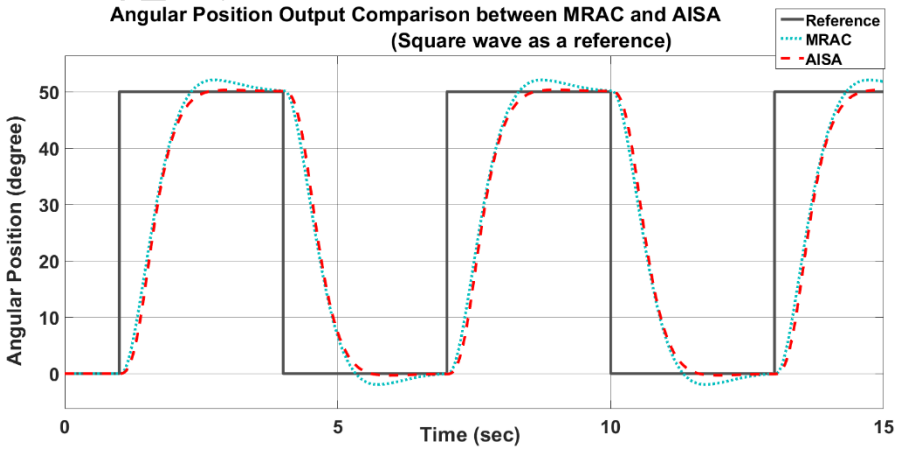

Fig. 19. The system response for Square Wave input considering MRAC and AISA technique.

Additionally, control signals originating from both the AISA controller and that of the MRAC controller are shown on Fig. 20. The analysis of these signals indicates that the control signal generated by the AISA controller is lower than that produced by the MRAC controller which, in turn, implies higher power efficiency. Overall, these figures show that AISA controller is more efficient and perform better in control applications.

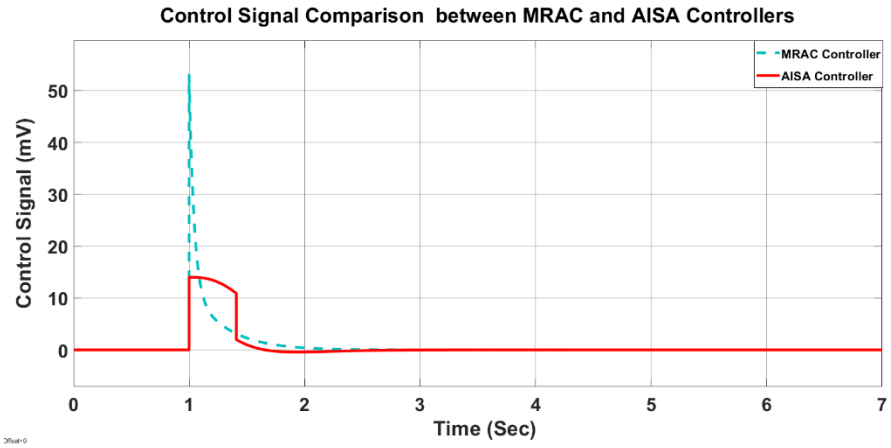

Fig. 20. The control signal considers MRAC and AISA techniques.

Also, Table 11 displays the differences in performance metrics of the robotic arm systems using AISA Control as well as MRAC Control. Some key performance indicators like rise time, settling or stabilization time, as well as middle peaks known as overshot are compared to determine how efficient each control strategy is. This comparison sheds more light on the dynamic behavior of the robotic arm in question as well as its stability under various control strategies used.

TABLE 11. SPECIFICATIONS OF THE AISA AND MRAC SYSTEMS.

Specification	AISA	MRAC
Rise Time	0.81337 Sec	0.8269 Sec
Settling Time	2.4071 Sec	3.2922 Sec
Peak	50 degrees	50 degrees
Peak Time	2.8782 Sec	2.7280 Sec

Overall, The AISA has great potential in the field of robotic control systems since it can decrease the time of response and the time of rise, minimizing overshoot, conserving energy and most importantly maintaining balance in motion. Owing to these advantages, AISA is likely to be useful in many robotic applications such as industrial robot, self-driving system and rehabilitative robotic system.

6. EXPERIMENTAL SETUP

This section involves the development and implementation of an experimental setup to test and assess control algorithms as illustrated in Fig. 21. A single-joint robotic arm weighing 0.85 kg was assembled based on a brushed DC motor from Shenzhen Feetech RC Model Co., Ltd, its characteristics being mechanical inertia J_m = 0.018 kg·m^2 and torque constant k_t = 9 kg·cm/A. The reference position of the arm in this instance was set at the horizontal position, which corresponded to an angular position of 0 degrees, and thus remained consistent throughout all the experiments conducted. The arm position was measured by a carbon film potentiometer of 220-degree angle which was attached to the DC motor shaft via copper gears. The output response was measured by a PeakTech P 1337 oscilloscope which has 100 MHz and 2 channels specifications.

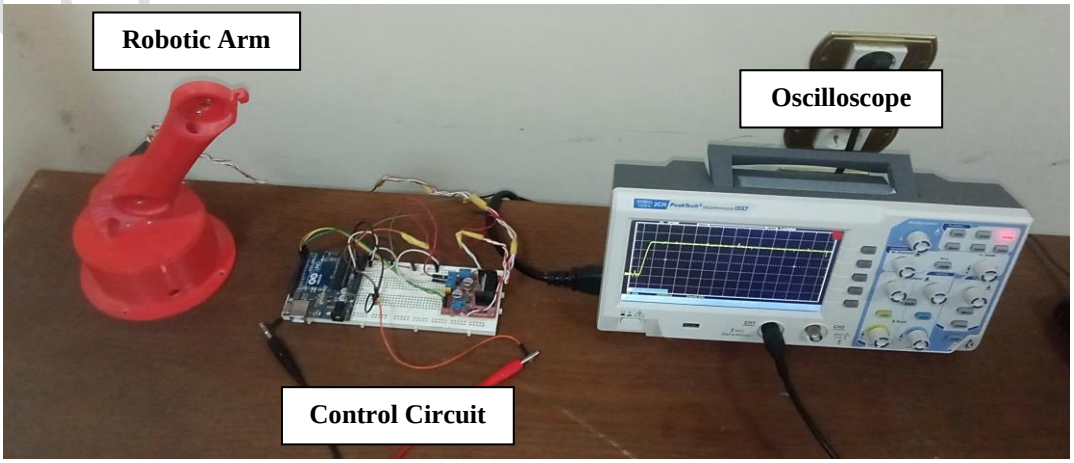

Fig. 21. Experimental Setup of Robotic Arm Model and Control Circuit.

The control circuitry was developed and implemented through Arduino IDE 1.8.20 programming environment as well as Arduino C programming language for accurate and effective control of the robotic arm position. In addition, Fig. 22 shows the block diagram of the robotic arm model and its control circuit, which outlines the system architecture in detail. This setup allowed different control techniques to be explored and how they affected the positioning accuracy and stability of the arm.

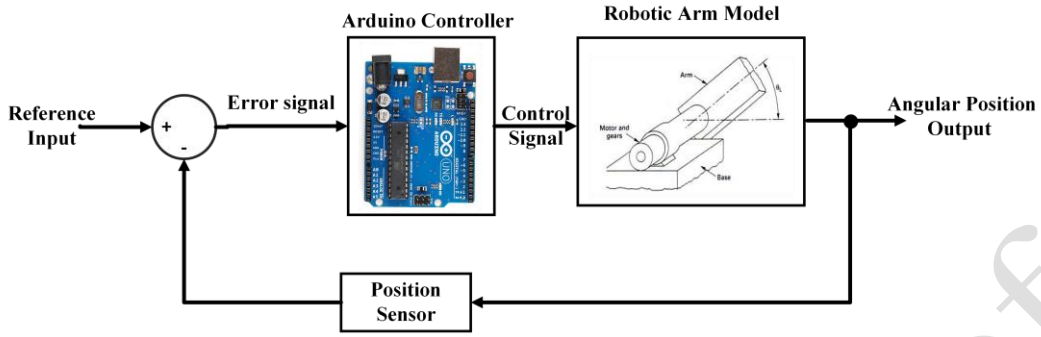

Fig. 22. Block diagram of the Robotic arm model and Control Circuit.

The control circuit is composed of an Arduino Uno microcontroller for programming and the L298N motor driver for controlling the motor rotation speed. The zoomed-in view of the control circuit associated with the robotic arm is provided, showing the key components and their connections is presented on Fig. 23.

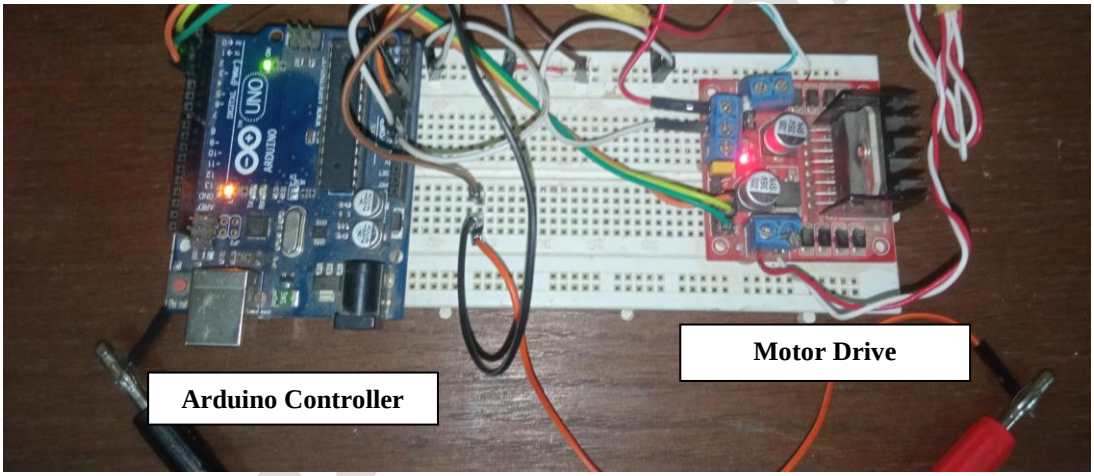

Fig. 23. Control Circuit of the Model.

The experimental output response of the AISA controller and conventional PID controller as taken from oscilloscope screen is presented in Fig. 24.

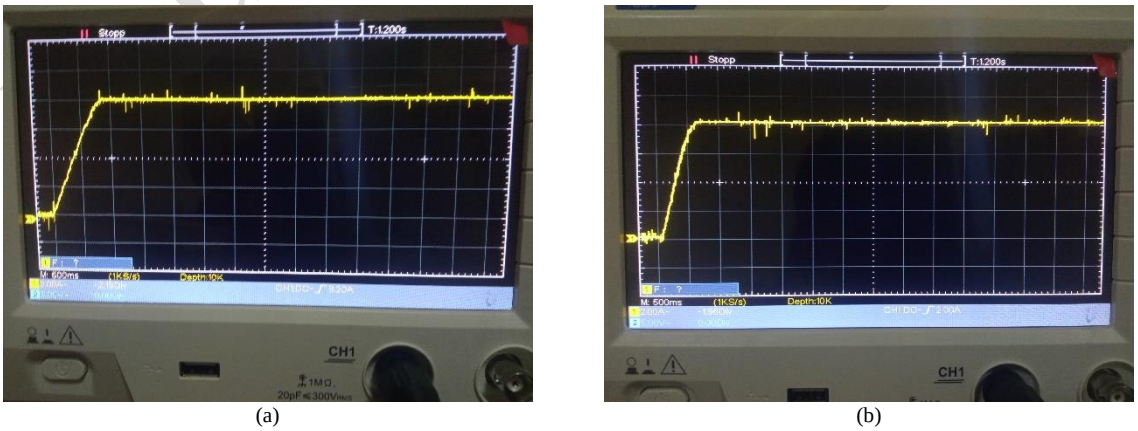

(a) (b)

Fig. 24. Oscilloscope Output for Angular Position Response of (a) Conventional PID Controller, (b) AISA Controller.

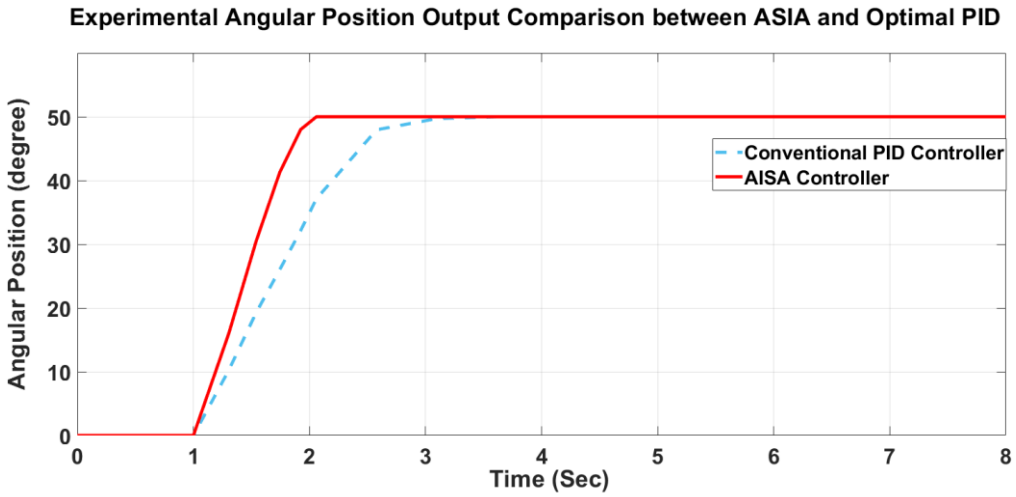

Fig. 25. Experimental Comparison of the Angular Position Response of a Conventional PID Controller and Approaching Index Switching Controller.

Fig. 25. illustrates the experimental angular position output response results for both the conventional PID controller and the AISA controller. The corresponding responses are plotted using MATLAB, with both signals displayed on the same figure for comparison. It can be seen that AISA is superior when rise time and settling time are considered. The conventional PID system takes about 2 s to stabilize, while the approach index switching system takes approximately 0.9 s to stabilize its output response. This better output performance in terms of time of the control system portrayed shows how the control algorithm was able to enhance the control of the robotic arm to a higher degree.

7. CONCLUSIONS

The concept of Approaching Index Switching Algorithm (AISA) is one of the methods of control strategies in which two controllers are used to obtain a desired response very fast without overshooting and yet ensuring that the system is still stable. The findings indicated that AISA was better than standard PID, Optimal PID, FOPID, and MRAC which are based on PID controllers. This capability of the method under consideration to control the levels of control signals also helps to achieve considerable energy efficiency whereby robotic arms can work twice faster than the usual operation with lower energy input.

This article addresses the major challenges in the design of control systems for industrial robotic arms by proposing a method of control enhancement that involves the dynamic switching of P and PID controllers leading to better performance, faster response, and lower power consumption. careful tuning of the switching index is essential, as over or under-tuning may lead to oscillations or let the system become unstable completely. Further, this strategy may not be effective when applied to systems with a high level of model uncertainty. AISA, nonetheless, remains a viable approach for controlling a robotic arm concerning its accuracy.

Results obtained from experiments along with simulations show that the Approaching Index Switching Algorithm (AISA) has a quicker response than control strategies such as Conventional PID, Optimal PID, FOPID and MRAC controllers in terms of accuracy and efficiency. AISA achieves low settling and rise times hence it guarantees better dynamic performance. It also possesses zero overshoots, which is essential for accurate positioning, and it keeps the control signal at a reasonable level improving the energy efficiency and stability of the system. Clearly, these advantages show that AISA can be considered a superior control scheme for controlling a robotic arm than traditional and advanced control methods.

For future research, applying AISA techniques to multi-joint robotic structures as well as investigating the possibility of switching among different controller types will be available. The results will enhance the performance and flexibility of industrial robots. To summarize, this study has proved that AISA is a viable control strategy in the context of industrial arm manipulation. Moreover, AISA offers improvement in both operational efficiency, reliability of the technology, and lower electricity consumption facilitating AISA's wide possibilities of implementation in industries that demand high precision and speed. The advances in the field of robotic systems are in line with the aspirations of our study, which is geared towards creating better and more effective control systems for that matter, in the muscle of turning better ideas into real products in the market.

References

[1] Y. H. T. Htun, M. S. Hlaing, and T. T. Hla, "Master-Slave Synchronization of Robotic Arm using PID Controller," *Indonesian Journal of Electrical Engineering and Informatics*, vol. 11, no. 1, 2023.

[2] P. Sutyasadi, "Control Improvement of Low-Cost Cast Aluminium Robotic Arm Using Arduino Based Computed Torque Control," *Jurnal Ilmiah Teknik Elektro Komputer dan Informatika*, vol. 8, no. 4, 2022.

[3] F. Moulahcene, H. Laib, and A. Merazga, "Angular Position Control of DC Gear-Motor Using PID Controllers for robotic Arm," in *International Conference on Electrical, Computer, and Energy Technologies, ICECET 2022*, 2022.

[4] F. A. Salem, "Modeling, Simulation and Control Issues for a Robot ARM; Education and Research (III)," *International Journal of Intelligent Systems and Applications*, vol. 6, no. 4, 2014.

[5] B. A. Bazzi and N. G. Chalhoub, "Fuzzy sliding mode controller for a flexible single-link robotic manipulator," *JVC/Journal of Vibration and Control*, vol. 11, no. 2, 2005.

[6] M. Z. Bin Abdul Karim and N. M. Thamrin, "Servo Motor Controller using PID and Graphical User Interface on Raspberry Pi for Robotic Arm," in *Journal of Physics: Conference Series*, 2022.

[7] S. A. Al-Samarraie and I. I. Gorial, "Modeling of Electromechanical System and Motion Control for Mechatronics Application," *International Review of Automatic Control*, vol. 16, no. 5, 2023.

[8] W. W. Naing, K. Z. Aung, and A. Thike, "Position Control of 3-DOF Articulated Robot Arm using PID Controller," *International Journal of Science and Engineering Applications*, vol. 7, no. 9, 2018.

[9] R. Agrawal, K. Kabiraj, and R. Singh, "Modeling a Controller for an Articulated Robotic Arm," *Intelligent Control and Automation*, vol. 03, no. 03, 2012.

[10] M. M. Maung, M. M. Latt, and C. M. Nwe, "DC Motor Angular Position Control using PID Controller with Friction Compensation," *International Journal of Scientific and Research Publications (IJSRP)*, vol. 8, no. 11, 2018.

[11] L. S. Mezher, "Position control for dynamic DC MOTOR with robust PID controller using MATLAB," *International Journal of Advanced Trends in Computer Science and Engineering*, vol. 8, no. 3, 2019.

[12] A. Ma'arif and A. Çakan, "Simulation and arduino hardware implementation of dc motor control using sliding mode controller," *Journal of Robotics and Control (JRC)*, vol. 2, no. 6, 2021.

[13] D. Effiong Oku, E. Patrick Obot, C. Author, and D. Effiong Oku, "Comparative Study Of PD, PI And PID Controllers For Control Of A Single Joint System In Robots," *The International Journal of Engineering and Science (IJES)*, vol. 7, no. 9, pp. 51–54, 2018.

[14] Nafiseh Ebrahimi, "Modeling, simulation and control of a robotic arm," *engrxiv.org*, 2019.

[15] D. Singh Rana and A. Professor, "Modelling, stability analysis and control of flexible single link robotic manipulator," 2007.

[16] M. Rohman and D. I. Saputra, "Modeling and Controlling the Actuator Joint Angle Position on the Robot Arm Base Using Discrete PID Algorithm," *Ultima Computing : Jurnal Sistem Komputer*, vol. 13, no. 2, 2021.

[17] Nihad Wazzan A.Basil N.Raad M.Kasim Mohammed H, "PID Controller with Robotic Arm using Optimization Algorithm," *International Journal of Mechanical Engineering Education*, 2022.

[18] M. A. Rashidifar, A. A. Rashidifar, and D. Ahmadi, "Modeling and Control of 5DOF Robot Arm Using Fuzzy Logic Supervisory Control," *IAES International Journal of Robotics and Automation (IJRA)*, vol. 2, no. 2, 2013.

[19] T. M. Ahmed, A. N. A. E. Gaber, R. Hamdy, and A. S. Abdel-Khalik, "Position Control of Arm Manipulator within Fractional Order PID Utilizing Particle Swarm Optimization Algorithm," in *IEEE Conference on Power Electronics and Renewable Energy, CPERE 2019*, 2019.

[20] A. Ashagrie, A. O. Salau, and T. Weldcherkos, "Modeling and control of a 3-DOF articulated robotic manipulator using self-tuning fuzzy sliding mode controller," *Cogent Eng*, vol. 8, no. 1, 2021.

[21] T. Seghiri, S. Ladaci, and S. Haddad, "Fractional order adaptive MRAC controller design for high-accuracy position control of an industrial robot arm," *International Journal of Advanced Mechatronic Systems*, vol. 10, no. 1, 2023.

[22] W. A. Shatnan, M. D. Hashim Almawlawe, and M. A. Al-Aress Jabur, "Optimal Fuzzy-FOPID, Fuzzy-PID Control Schemes for Trajectory Tracking of 3DOF Robot Manipulator," *Tikrit Journal of Engineering Sciences*, vol. 30, no. 4, 2023.

[23] W. Lv, D. Li, S. Cheng, S. Luo, X. Zhang, and L. Zhang, "Research on PID control parameters tuning based on election-survey optimization algorithm," in *2010 International Conference on Computing, Control and Industrial Engineering, CCIE 2010*, 2010.

[24] O. Djaneye-Boundjou, X. Xu, and R. Ordonez, "Automated particle swarm optimization based PID tuning for control of robotic arm," in *Proceedings of the IEEE National Aerospace Electronics Conference, NAECON*, 2016.

[25] S. R. Tawfeic "The Approaching Index Switching Algorithm" 7th International Conference on Intelligent Engineering Systems, INES 2003, March 4- 6 Assiut Egypt, 2003.

[26] S. R. Tawfeic, "Track seeking control for hard disk drives using the approaching index switching algorithm," in *Proceedings of the International Conference on Computer and Communication Engineering 2008, ICCCE08: Global Links for Human Development*, 2008.

[27] M. Vaijayanti, "Robotic Arm Control Using Pid Controller and Inverse Kinematics," *International Journal of Engineering Development and Research*, vol. 5, no. 2, 2017.

[28] A. Sathish Kumar *et al.*, "An intelligent fuzzy-particle swarm optimization supervisory-based control of robot manipulator for industrial welding applications," *Sci Rep*, vol. 13, no. 1, 2023.

[29] A. T. Jawad, H. M. Gheni, N. J. Abed, N. S. Ali, and A. N. Abdullah, "Design of adaptive controller for robot arm manipulator based on ANN with optimized PID by PSO algorithm," in *AIP Conference Proceedings*, 2023.

[30] Y. K. Soni and R. Bhatt, "Simulated Annealing optimized PID Controller design using ISE, IAE, IATE and MSE error criteria," *International Journal of Advanced Research in Computer Engineering & Technology*, vol. 2, no. 7, 2013.

[31] A. K. M and R. Younus Fadhil, "Performance Improvement of the Robotic Arm using Fractional Order PID," *Engineering and Technology Journal*, vol. 34, no. 14, 2016.

[32] D. Zhang and B. Wei, "A review on model reference adaptive control of robotic manipulators," 2017.